RESEARCH ARTICLE

INTERNATIONAL RESEARCH JOURNAL OF MULTIDISCIPLINARY TECHNOVATION

Asian Research Association

DOI: 10.54392/irjmt25323

Mustum (extracted grape juice) - Assisted Green Synthesis of Metal Oxide Nanoparticles: Evaluation of Phase, Vibrational, Morphological, and Thermal Properties

S.J. Nilofur Fathima [a], C. Arun Paul [b], K. Mathu Metha [a], E. Ranjith Kumar [a, *]

[a] Department of Physics, KPR Institute of Engineering and Technology, Coimbatore, 641407, Tamil Nadu, India.

[b] Department of Science and Humanities, Sri Krishna College of Engineering and Technology, Coimbatore-641008, Tamil Nadu, India.

* Corresponding Author Email: ranjueaswar@gmail.com

DOI: https://doi.org/10.54392/irjmt25323

Received: 06-11-2024; Revised: 14-05-2025; Accepted: 21-05-2025; Published: 28-05-2025

Abstract: Environmentally friendly green chemical techniques for nanomaterial synthesis employing non-toxic chemicals and renewable resources have received interest. The green chemical method was adopted to synthesize metal oxide nanoparticles to study their physicochemical properties. XRD was used for crystallite size, lattice characteristics, and phase purity. XRD analysis confirmed that the metal oxide nanoparticles produced are single-phase cubic (NiO and Co_3O_4) and monoclinic (CuO) with 25–35 nm crystallite diameters. Fourier-transform infrared spectroscopy (FTIR) has been used to study functional groups and chemical bonding on metal oxide nanoparticle surfaces. A detected peak between 600 and 400 cm-1 indicates Metal-Oxygen in the synthesized metal oxide nanoparticles. FESEM and TEM were used to investigate nanomaterials' surface morphology, particle size, and shape at high resolution. TGA was used to evaluate metal oxide nanoparticle heat stability and degradation. Two large weight losses at 100°C and above 550°C suggest water and other sample constituents are eliminated. The antibacterial study shows good efficacy in Co_3O_4. The results demonstrate that synthesized nanoparticles can be used in many functional applications.

Keywords: Mustum (Grape Juice), Green Chemical Synthesis, Metal Oxides, TEM

1. Introduction

Recently, green chemical synthesis has been defined as an environmentally friendly method that is essential for synthesizing metal oxides since the biological component acts as a capping and reducing agent, which would affect the total chemical processes that take place throughout the research [1-4]. Green chemical synthesis is a novel and ecologically sustainable technique for creating metallic nanoparticles [5]. This method greatly reduces the environmental impact of producing nanoparticles by using natural resources such microbes, biopolymers, and plant extracts as stabilizing and reducing agents [6-7] This method eliminates the need for external experimental conditions, such as high temperatures or pressures required in conventional techniques like chemical vapor deposition, as this unique method is a more accessible choice [8–13] This approach has many benefits, such as being naturally simple, being extremely cost-effective, producing non-toxic byproducts, being efficient in terms of time consumption, being strongly aligned with environmentally friendly practices, and having the promising potential for seamless scalability, which makes it appropriate for large-scale production endeavors [14–18]. A large family of compounds known as metal oxides is produced when metals and oxygen come together. Hydrated oxides, simple oxides, and oxyhydroxides are some of the groups into which they may be divided [19]. This categorization reflects the complexity of their structures and the presence of other functional groupings that may influence their traits and responsiveness. Metal oxides are branched into primary minerals and secondary minerals. Iron, aluminum, and manganese secondary oxides in particular are very reactive due to their large specific surface area. Their strong reactivity makes them indispensable to many chemical processes since it allows them to interact effectively with many environmental conditions which understand how metal oxides behave in natural systems, one must have a solid understanding of their composition and structure [20–25]. Their production and properties are greatly influenced by environmental factors including pH and temperature, which also affects how well they work in different applications [26] recently, metal oxides have been produced using this environmentally friendly synthesis technique. Jyoti

Yadav *et al.* [27] generated iron nanoparticles to remove heavy metals from aqueous solution using syzygium aromaticum. A remarkable adsorption capacity was observed while extracting Cr (VI) ions from water, and it was crystalline. These results demonstrate how efficient, long-lasting, and ecologically safe this approach is for treating wastewater and heavy metal pollution. Ansari Maria *et al*., 2024 [28] used a green synthesis method to analyze crystalline copper nanoparticles using sodium borohydride reduction for enhanced gas sensing applications. The results show the resistivity values of the copper conductive films showing 4.1 × 103 Ω cm, 8.8 × 10-2 Ω cm, and 1.4 × 10-5 Ω cm in various atmospheric environments, specifically nitrogen gas, and hydrogen gas, respectively. The green synthesis of copper oxide nanoparticles using Amaranthus dubius leaf extract demonstrates promising potential for sensor and photocatalytic applications [29]. From these various green fuels assisted green synthesis, we have selected mustum (filtered grape juice). The choice of mustum in the present study is highly supported by the presence of a wide range of chemical components in its juice like isoflavones, flavanols, furanocoumarins and anthocyanidin [30]. The presence of essential chemical components with high density of hydroxyl groups which are phytochemicals have the properties like reducing, capping and stabilizing agents; hence they can be highly useful to control the size and shape during the synthesis of nanostructured material [31]. These chemical constituents of grapefruit juice can have the ability to tune the morphology, electronic structure, create defects, and enhance the catalytic function. It is noteworthy to mention that tartaric acid is naturally present in grapes, thereby highlighting its availability and potential applications in various fields [32-36]. The concentration range of tartaric acid in fresh grape mustum typically lies between 0.4% to 0.9% by weight. The agglomeration of nanoparticles can be controlled by tartaric acid which acts as a stabilizing agent that leads for better dispersion in various matrices, which makes applications like coatings, catalysis, and sensors more crucial. This tartaric acid aids in binding metal ions such as copper, iron or zinc by acting as a chelating agent and also wards off premature precipitation as it allows stabilization by controlling nanoparticle synthesis that induces enhanced stability and sustainability. Due to these benefits, it is a helpful building block in the as biofuel for multiple applications, ranging from biosensors to biomedical devices. Tartaric acid assisted synthesis of metal oxide nanoparticles usually demonstrates higher catalytic behavior. The controlled size and high surface area provide more active sites for catalysis.

2. Materials and Synthesis

The experiment is conducted using metal oxides such as CuO, NiO and Co_3O_4, using mustum (filtered grape juice) as a biofuel.

2.1. Preparation of grape extract

Fresh grapes were purchased from the Kambam valley of Theni district, Tamil Nadu which is known as *"the Grape City of South India"*. A 100g of grapes were washed thrice with clean fresh water to remove any impurities and dirt present on the surface. The grapes were carefully crushed to extract fresh grape juice called mustum. The first stage of the winemaking process. Then the obtained extract was filtered to remove the skin, seeds and stem. Later the resultant filtered mustum was utilized as an assisting fuel for the green synthesis process.

2.2. Method of synthesis

A 25 ml of filtered mustum was taken and mixed with 25 ml of distilled water. The resulting mixture was stirred with a magnetic stirrer at 810 – 850 rpm for about 30 minutes. A quantity of 6.040 g of Copper (II) nitrate trihydrate [Cu $(NO_3)_2.3H_2O$] of blue colour is taken. It is mixed with 50 ml of distilled water and stirred with a magnetic stirrer for 10 minutes speed ranging to 500 rpm. Later mustum solution and Copper (II) nitrate trihydrate solution are mixed for 10 mins at 1550 rpm. The resulting solution was poured into the 1000 ml glass beaker and placed in the hot place for combustion. Temperature is gradually increased and continuously stirred. Due to heat treatment, the solution started evaporating, releasing gas slowly leaving char behind. After combustion, the charr was collected and ground using a mortar and pestle. The final product, in the form of a powder, was gathered and stored in a vial and further required characteristics were taken. Then a similar producer was followed to prepare NiO and Co3O4 nanoparticles. Figure. 1 shows the schematic representation of the preparation of the sample. NiO nanoparticles were prepared from Nickel (II) nitrate hexahydrate [Ni $(NO_3)_2.6H_2O$], which has a weight equal to 7.2697 g while Co_3O_4 nanoparticles were synthesized from Cobalt (II) nitrate hexahydrate, [Co $(NO_3)_2.6H_2O$] has a weight equal to 7.2757 g in the identical procedure used.

2.3. Characterizations Technique

XRD analysis of the CuO, NiO, and Co_3O_4 prepared from filtered mustum was carried out to confirm structural properties using Bruker AXS D8 diffractometer equipped with the copper target; (wavelength = 1.5406 Å). FTIR Spectra Were Obtained Using a Fourier Transform Infrared Spectrometer (FTIR) Themo fisher Nicoletis10. Field-emission Scanning Electron Microscope (FESEM) (Gemini 300 SEM), and Transmission Electron Microscope (TEM) JEM-2100 Plus were used to study the surface morphology. The TG-DTA studies (PerkinElmer) were used to define the thermal characteristics.

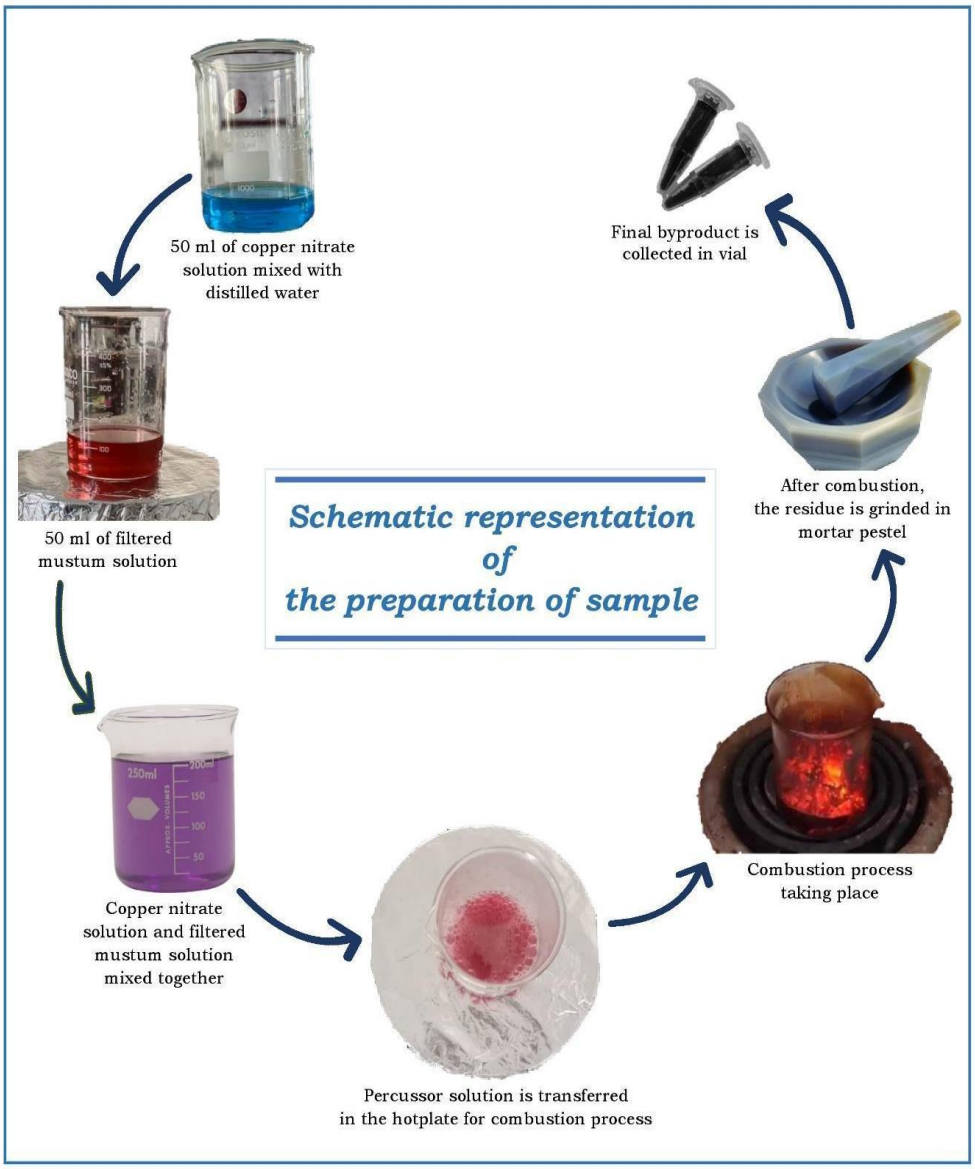

Figure 1. Displays the schematic representation of the preparation of the sample

The antibacterial test was conducted to study the antibacterial efficacy of the material.

3. Result and Discussion

3.1 XRD analysis

XRD, a powder diffraction technique is primarily used to find the crystal size of the sample. The sharp peaks symbolise the defined crystallization of metal oxides (Figure 2). In CuO, The XRD pattern confirmed a monoclinic structure (JCPDS 00-005-0661). The peaks with miller indices ranging (0,0,2), (1,1,1), (2,0,0), (-1,1,2), (1,1,2), (2,0,2), (-1,1,3), (0,2,2), (2,2,0), (3,1,1), (0,0,4) and (-2,0,4) are matched with JCPDS number. The maximum intensity peak was observed at 35°6. In NiO, it shows cubic structure that matched well the JCPDS number 04-006-6160. The peaks with the miller indices (1,1,0), (2,0,0), (1,1,1), (0,2,0), (0,2,1), (2,2,0) and (0,0,2) were matched with JCPDS number. The maximum intensity peak was observed at 43°3. In Co_3O_4, it shows cubic structure that matched well the JCPDS number 00-043-1003. The peaks with the miller indices (3,1,1), (2,2,2), (4,0,0), (3,3,1), (4,4,0), (5,3,1) and (6,2,2) were matched with JCPDS number. CuO has a crystallite size of 27 nm and a monoclinic structure, NiO has a crystallite size of 26 nm and a cubic structure, and Co_3O_4 has a crystallite size of 30 nm and a cubic structure. The maximum intensity peak was observed at 36°9. Debye Scherrer's equation was used to calculate the average crystallite size of these nanoparticles [39].

$$\boldsymbol{D} = \frac{K\lambda}{\beta Cos\theta} \quad (1)$$

were,

D - Average crystallite size,

K- Dimensionless shape factor with a value close to unity,

λ - Wavelength of the X-ray, β - Full width at half maximum intensity (FWHM) and

θ - Bragg angle.

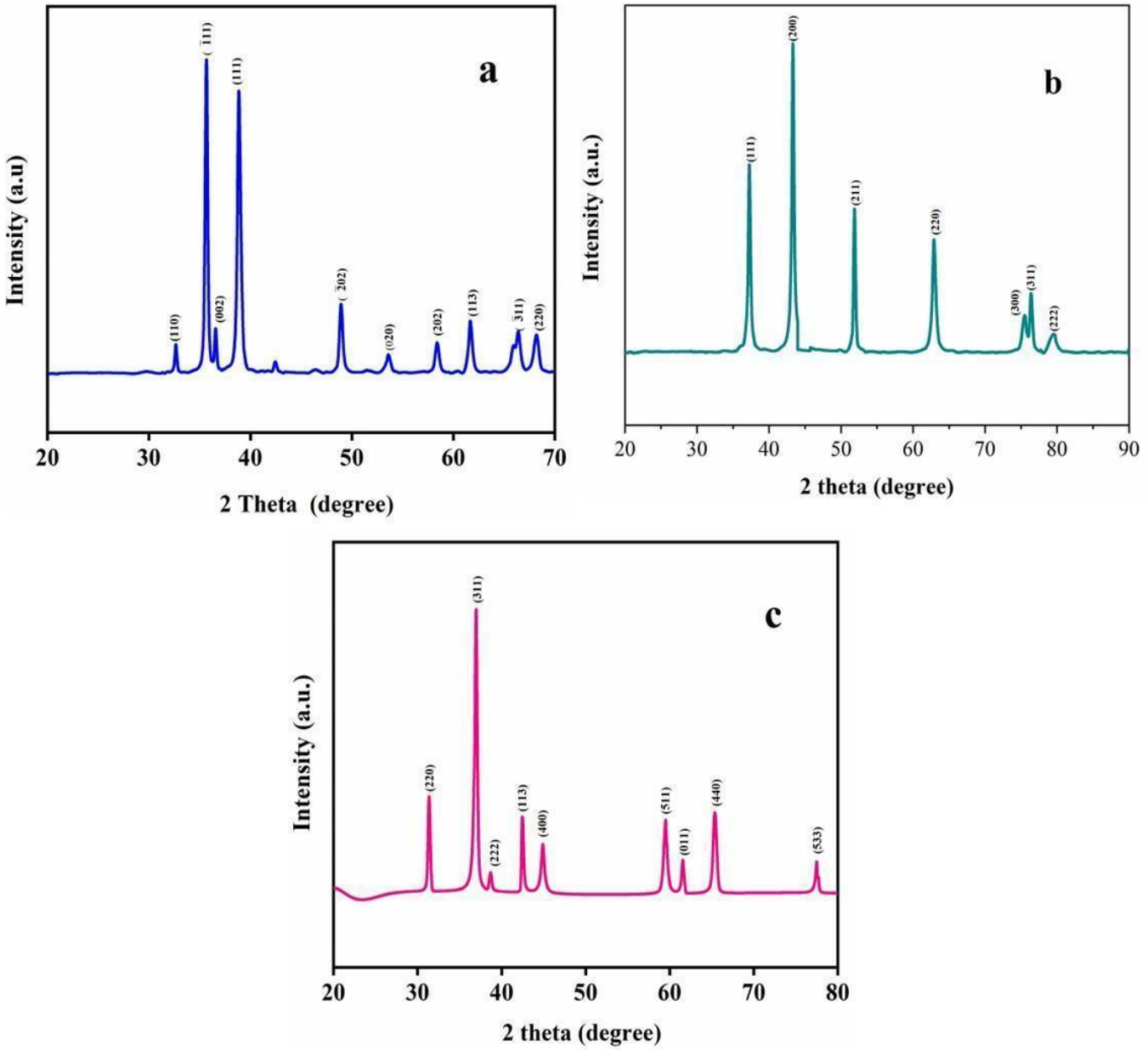

Figure 2. illustrates the XRD patterns of the metal oxides: (a) CuO, (b) NiO, and (c) Co_3O_4.

3.2. FTIR analysis

FTIR (Fourier-transform Infrared Spectroscopy) is used to analyse the chemical bonds and molecular structure. From the Figure. 3, CuO shows a peak range between 480-600 cm^{-1}. This peak is visible as one of the prominent absorptions in the lower wavenumber region due to the heavier mass of the copper atom and the nature of the metal-oxygen bond and another peak at 2189 cm^{-1} showing broad adsorption due to O-H stretching. In NiO, peaks observed at 424.31 cm^{-1} exhibiting strong peak indicating Ni-O bond stretching. Peak range between 570 cm^{-1} to 1970 cm^{-1} exhibits additional peak for Ni-O vibrations and H-O-H due to water, and absorption bands that correspond to this range. In Co_3O_4 the bending modes**,** occur when the bond angles between metal and oxygen ions change, leading to peaks at lower wavenumbers as 450 cm^{-1}. The stretching modes occur when the length of the Co-O bonds changes, leading to peaks at higher wavenumbers 550 cm^{-1} and 662 cm^{-1}, corresponds to Co–O stretching. These specific peaks would confirm the presence of Co_3O_4. [40]

3.3 EDAX analysis and Surface morphological analysis

The EDAX (Energy Dispersive X-ray Analysis) results provide the elemental composition of CuO, NiO, and Co_3O_4 nanoparticles synthesized using combustion with filtered mustum. In CuO (Figure 4 and Figure. 5a), the elemental composition of copper (Cu) is 68.5% and oxygen (O) is 31.5%. Figure. 5b confirms the elemental composition of nickel (Ni) is 63.2% and oxygen (O) is 36.8%. Figure 5c shows the elemental presence of cobalt (Co) is 73.6% and oxygen (O) is 26.4%.

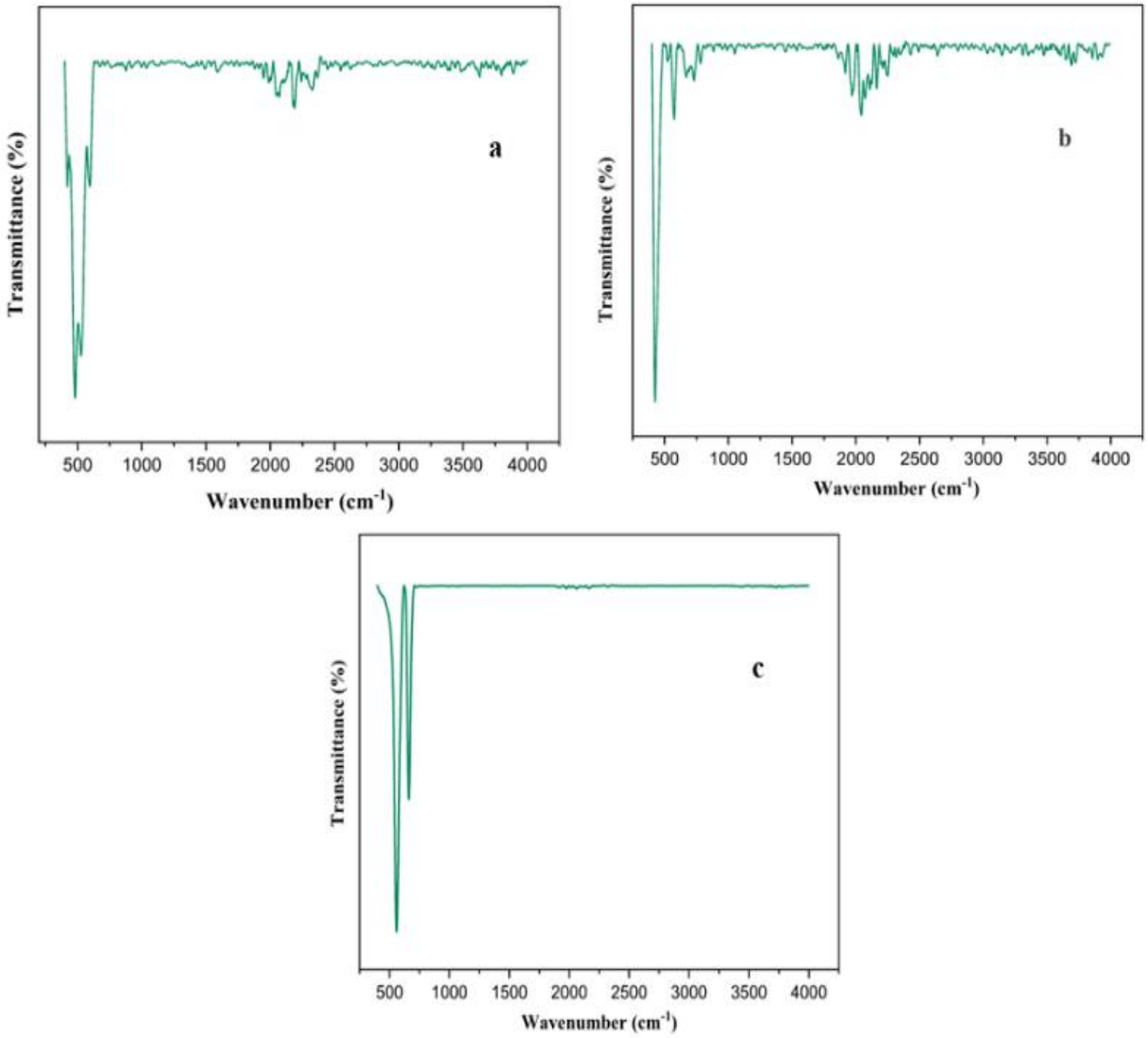

Figure 3. Depicts the FTIR spectra of the metal oxides: (a) CuO, (b) NiO, and (c) Co_3O_4.

These percentages represent the atomic composition of the elements in the nanoparticles, indicating a relatively pure formation of metal oxides [41]. Scanning electron microscope (SEM) used for imaging and analysing the surface structure and composition of materials at a very high magnification. SEM provides detailed images of the surface topography of a sample, allowing researchers to examine the surface features at the nanoscale. Figure. 6a shows the SEM image of the CuO which illustrates irregularly shaped particles with high porousness on a rough surface and shows a nano granular structure. This also indicates agglomeration as it minimizes the surface area which leads to high surface energy which is created due to rough and porous surface. Such morphology is often utilized in the field where high surface and reactivity are crucial [42]. Figure. 6b shows irregular clusters of NiO nanoparticles which are due to high surface energy. Factors such as conductivity and reactivity can be influenced due to aggregation and also exhibit significant porosity which exhibits nano clustered morphology. Figure. 6c exhibits thin, flake structure of Co_3O_4 nanoparticles. These thin flake structures are arranged in layer form which shows high surface area. This structure seems to be loosely packed, irregular in structure which shows non uniform distribution of particles. They can be utilized in performance enhancing applications such as catalysis, battery applications which could increase the charge storage capacity and reactivity of the materials [43].

3.4 Thermal analysis

TGA (Thermogravimetric Analysis) is a compositional technique that indicates loss of weight of the material in a controlled atmosphere with terms of temperature and time. This technique helps in composition, decomposition of material and determining thermal stability.

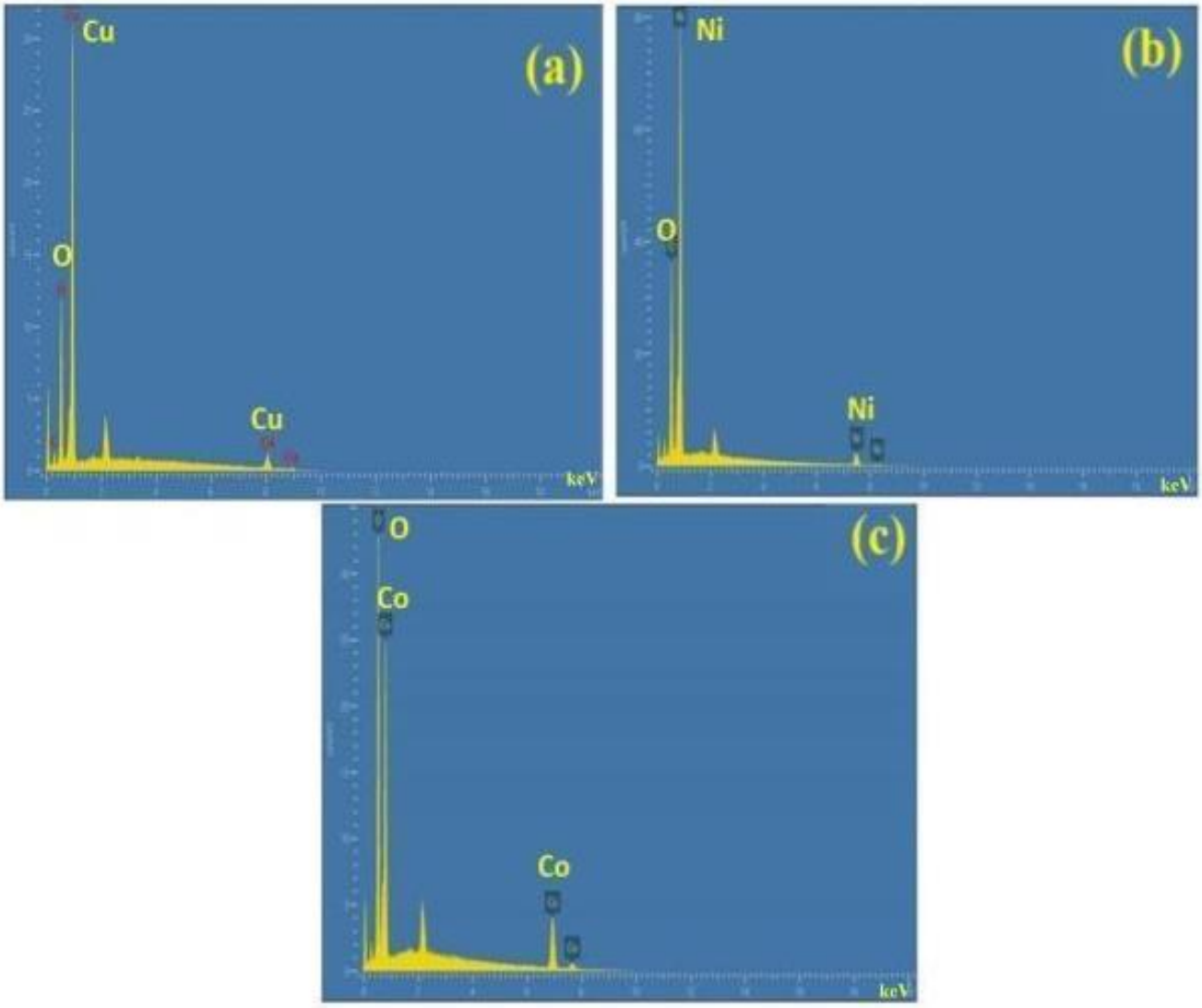

Figure 4. Presents the EDAX spectra of the metal oxides: (a) CuO, (b) NiO, and (c) Co_3O_4.

In the Fig. 6a shows the TGA graph of CuO, the loss of water and other volatile substances has taken place between 0°C - 400°C which is indicated by a blue curve. The blue curve shows a sharp weight loss at around 888.12°C. The derivative curve (red) shows a peak at this point, suggesting a rapid decomposition reaction. The peak is sharp, indicating that the decomposition happens within a narrow temperature range. The TGA curve shows a minor weight loss around 371.33°C with a corresponding derivative peak. This minor event could be due to the breakdown of another component or the release of water of hydration. At around 888.12°C, CuO experiences a significant weight loss, which may indicate the decomposition of the main material in CuO. In this graph of NiO (Figure. 6b), the material loses approximately 2.757% of its weight up to 1000°C. A significant transition occurs at around 295.11°C, with a moderate rate of weight loss (0.02543%/°C). The material is relatively stable between 400°C and 800°C. A slight decomposition starts again after 800°C. A gradual weight loss resumes after 800°C, as shown by the red curve (derivative weight) rising again. This indicates that the material starts to lose mass more slowly, which could be due to further decomposition or oxidation processes. Initially, in Co_3O_4 (Figure. 6c) weight loss occurred around 400°C about 15%. A specific event is indicated at 284.35°C with a derivative weight loss rate of 0.03497%/°C, suggesting some thermal decomposition or loss of volatile components. Between 400°C and 800°C, the weight loss curve remains relatively stable, indicating that the material is thermally stable in this range. This stability suggests that there is no significant decomposition or mass loss occurring in this temperature window. A sharp weight loss occurs at approximately 829.53°C. The derivative weight curve shows a significant peak at this point with a rate of 0.1672%/°C, indicating a rapid and substantial thermal decomposition. The material loses approximately 16.54% of its weight in this temperature range, which is a considerable amount, suggesting a major breakdown or reaction occurring in Co_3O_4. DTA measures the temperature difference between a sample and a reference material as they are heated or cooled under identical conditions.

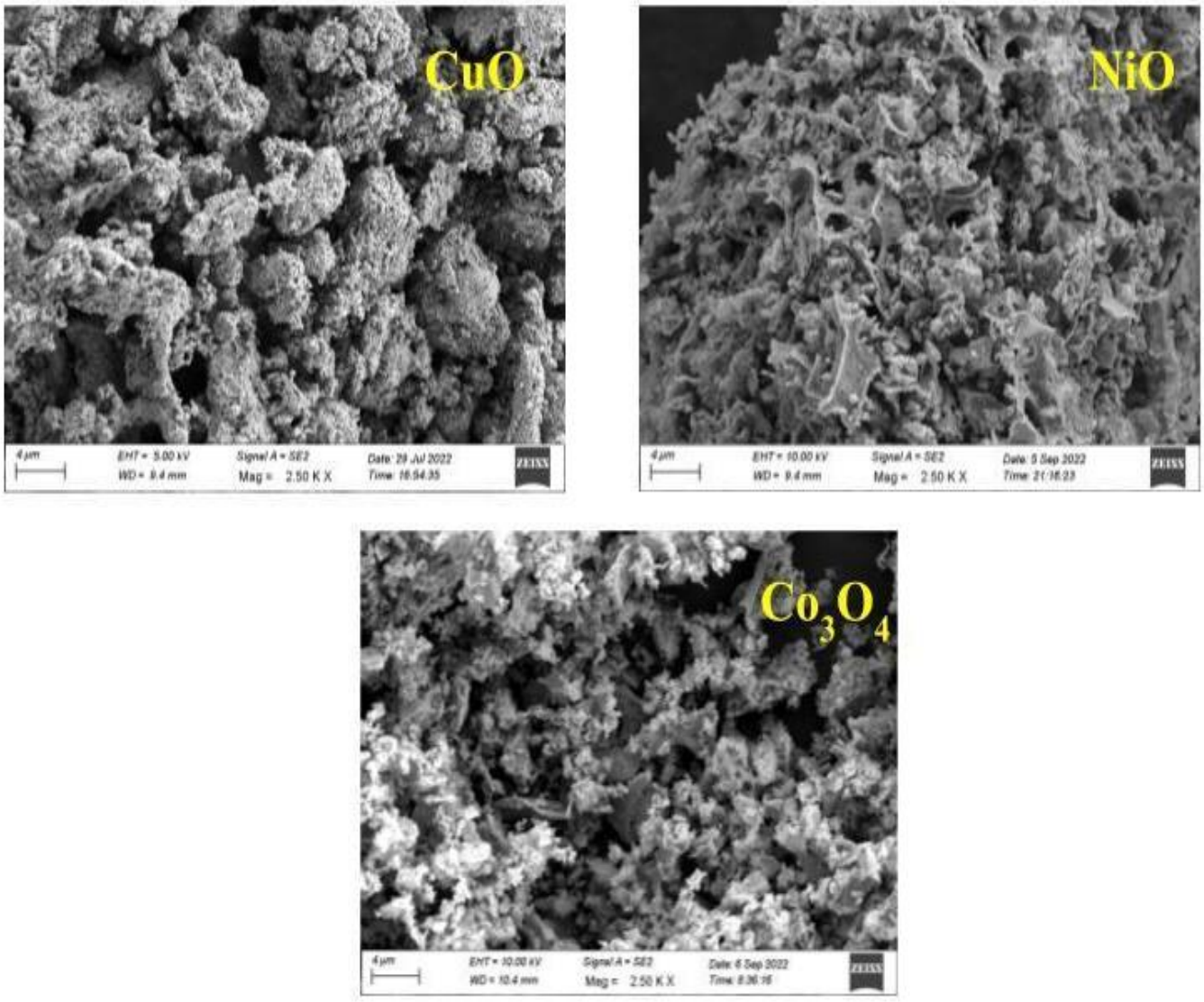

Figure 5. Displays the SEM micrographs of the metal oxides

This technique detects exothermic (heat-releasing) and endothermic (heat-absorbing) transitions in the sample. The above-mentioned graph, for both CuO and NiO, indicates an endothermic peak at lower temperatures suggesting solvent evaporation processes and organic decomposition. Co_3O_4 contains both endothermic and exothermic peaks. Endothermic peaks at lower temperatures are associated with solvent and organic component evaporation. Exothermic peaks indicate the crystallization and formation of Co_3O_4.These results suggest that the combustion synthesis with wine leads to the formation of metal oxides (CuO, NiO, and Co3O4) through a series of thermal decomposition steps, as indicated by the TG/DTA curves. The precise temperature ranges and peak characteristics provide insights into the thermal stability and decomposition behaviour of the precursor materials used in the synthesis [44].

3.5 Antibacterial Study

The method used here is the agar well diffusion method with Mueller-Hinton Agar (MHA). The bacteria used are Staphylococcus aureus, a Gram-positive bacterium commonly found in infections, and Pseudomonas aeruginosa, a Gram-negative bacterium. The zones of inhibition (mm) for CuO, NiO, and Co_3O_4 against gram-positive and gram-negative were measured at concentrations of 1 mg/ml, 2 mg/ml, and 3 mg/ml along with the antibiotic *Streptomycin.*

The antibacterial activity against *Staphylococcus aureus* (Gram-positive) of metal oxides nanoparticles shown in Figure 7. A higher concentration of nanoparticles exhibits noticeable antibacterial activity against *Staphylococcus* aureus than standard antibiotics. The incubation zone of NiO nanoparticles is comparatively better than the other metal oxide nanoparticles. The incubation zone at higher concentration of metal oxide nanoparticles is 3.33 mm at 3 mg/ml for CuO, 5.33 mm at 3 mg/ml for NiO and 2.67 mm at 3 mg/ml for Co_3O_4 respectively. CuO and Co_3O_4 nanoparticles performs better than antibiotic only at higher concentration.

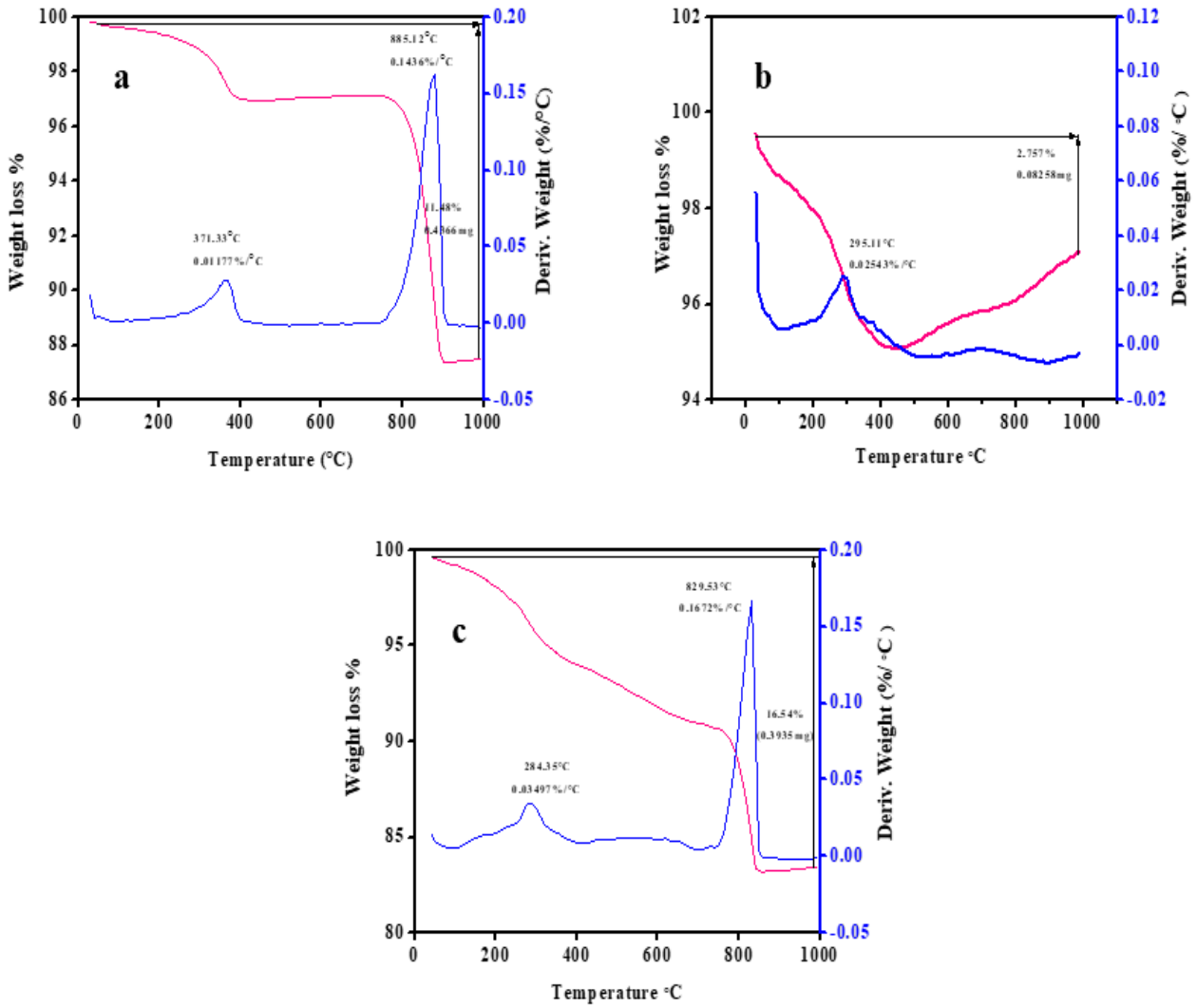

Figure 6. Illustrates the TG/DTA graphs of metal oxides: (a) CuO, (b) NiO, and (c) Co_3O_4.

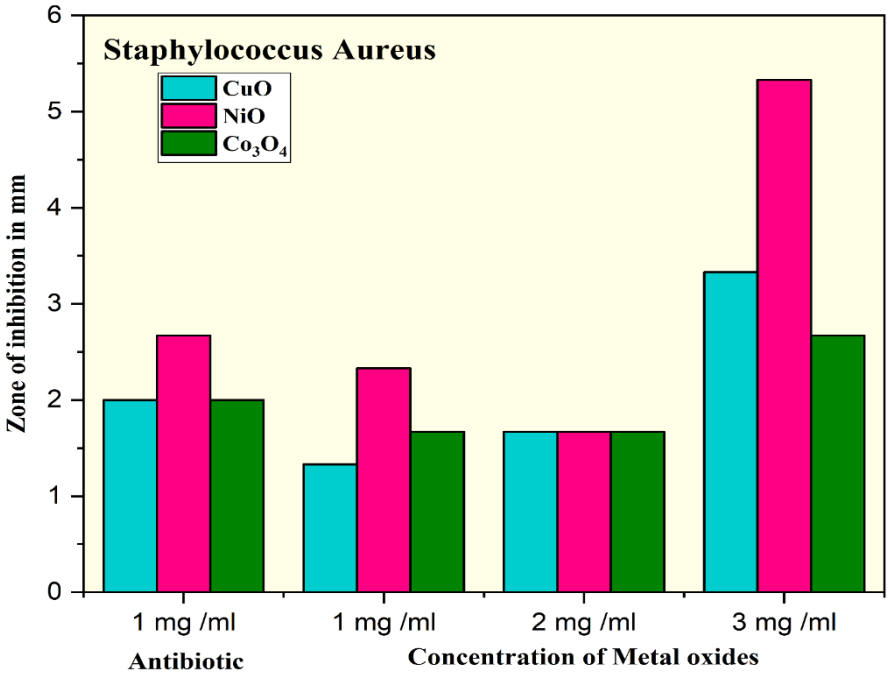

Figure 7. Shows the antibacterial activity of metal oxides against Staphylococcus aureus

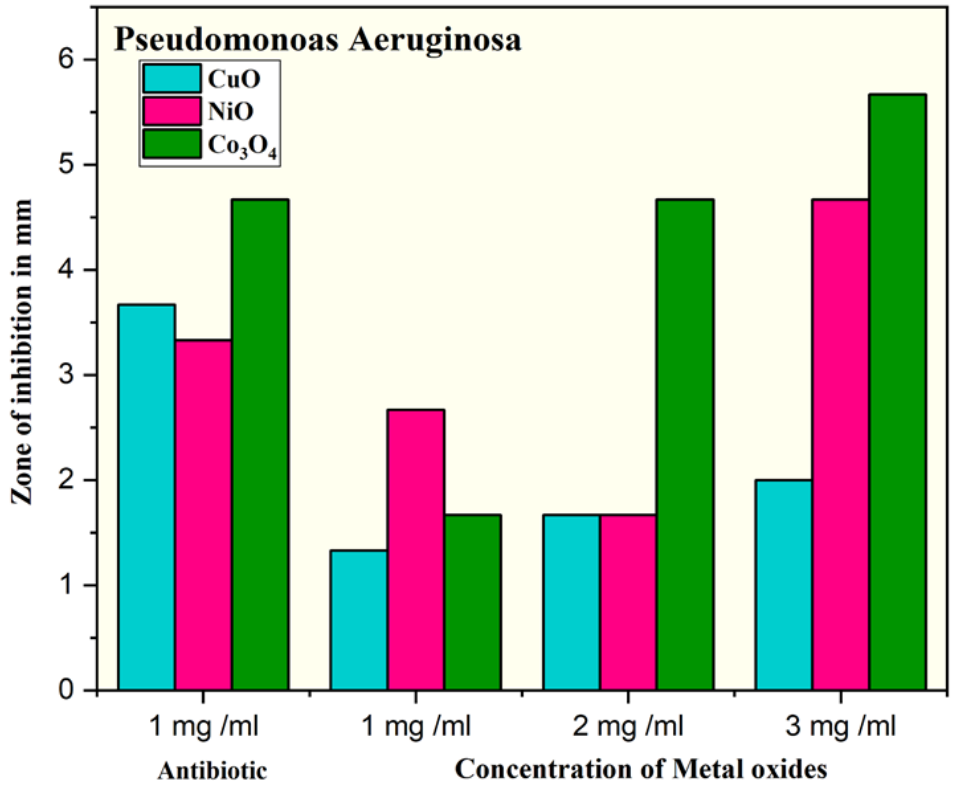

Figure 8. Depicts the antibacterial activity of metal oxides against Pseudomonas aeruginosa

Figure 8 illustrates the antibacterial efficacy of metal oxide nanoparticles against *Pseudomonas aeruginosa* (Gram-negative). Similarly to *S. aureus*, higher concentration of metal oxide nanoparticles shows increased antibacterial efficacy against *P. aeruginosa*. The incubation zone of Co_3O_4 demonstrates better efficacy even at a concentration of 2 mg/ml, exceeding CuO and NiO. The incubation zone at higher concentrations of metal oxide nanoparticles measures 1.67 mm for CuO at 3 mg/ml, 4.67 mm for NiO at 3 mg/ml, and 5.67 mm for Co_3O_4 at 3 mg/ml. In this instance, CuO and NiO exhibit better antimicrobial efficacy compared to greater doses. *P. aeruginosa* exhibited significantly more reliable natural resistance to both antibiotics and metal oxides than S. aureus.

4. Conclusion

Eco-friendly green chemical methods for nanomaterial synthesis utilizing non-toxic substances and renewable resources have garnered attention. This work primarily focuses on the physicochemical characteristics of metal oxide nanoparticles generated using green chemistry using grape juice. This process produced pure nanoparticles of CuO (monoclinic), NiO, and Co_3O_4 (cubic) that are 25–35 nm in size, as confirmed by XRD. FTIR detected the metal-oxygen connections in the range of 400–600 cm^{-1}, and EDAX confirmed the amounts of each element: Cu (68.5%), O (31.5%), Ni (63.2%), O (36.8%), and Co (73.6%), O (26.4%), showing very few impurities. SEM showed that CuO and NiO had rough, clumped shapes, while Co_3O_4 had thin, layered flakes with a large surface area. The TGA profiles showed two stages of degradation. The removal of water and volatile substances caused the first stage of degradation, which involved weight loss at temperatures below 400°C. The high-temperature breakdown confirmed the materials' thermal stability, with Co_3O_4 exhibiting the reliable stability (16.5% weight loss). The antibacterial activity against metal oxide nanoparticles with higher concentrations, than the antibiotic of 1 mg/ml, Co_3O_4 and NiO demonstrating better performance compared to CuO. Among these, NiO showed the highest efficacy against Gram-positive bacteria, while Co_3O_4 was most effective against Gram-negative strains. This eco-friendly approach aligns with better purity, thermally stable nanoparticles with tunable morphologies, making them promising for antimicrobial coatings. Due to their size-dependent property, nanoparticles can be used for catalysis, which can provide good surface area, tunable electronic properties, shape and size control, and sensor applications.

References

[1] S. Demarema, M. Nasr, S. Ookawara, A. Abdelhaleem, New insights into green synthesis of metal oxide based photocatalysts for photodegradation of organic pollutants: A bibliometric analysis and techno-economic evaluation. Journal of Cleaner Production, 463, (2024) 142679. https://doi.org/10.1016/j.jclepro.2024.142679

[2] J. Gubitosa, V. Rizzi, A. Laurenzana, F. Scavone,

E. Frediani, G. Fibbi, F. Fanelli, T. Sibillano, C. Giannini, P. Fini, P. Cosma, The “end life” of the grape pomace waste become the new beginning: The development of a virtuous cycle for the green synthesis of gold nanoparticles and removal of emerging contaminants from water. Antioxidants, 11(5), (2022) 994. https://doi.org/10.3390/antiox11050994

[3] G. Brahmachari, (2021) Green synthetic approaches in organophosphorus chemistry: recent developments. Organophosphorus Chemistry. https://doi.org/10.1039/9781839163814-00467

[4] J.A.Kumar, T. Krithiga, S. Manigandan, S. Sathish, A.A.Renita, P. Prakash, B.S. Naveen Prasad, T.R. Praveen Kumar, M. Rajasimman, A. Hosseini-Bandegharaei, D. Prabu, S. Crispin, A focus to green synthesis of metal/metal based oxide nanoparticles: Various mechanisms and applications towards ecological approach. Journal of Cleaner Production, 324, (2021) 129198. https://doi.org/10.1016/j.jclepro.2021.129198

[5] M.I. Benitez-Salazar, V.E. Niño-Castaño, R.A. Dueñas-Cuellar, L. Caldas-Arias, I. Fernández, J.E. Rodríguez-Páez, Chemical synthesis versus green synthesis to obtain ZnO powders: Evaluation of the antibacterial capacity of the nanoparticles obtained by the chemical method. Journal of Environmental Chemical Engineering, 9(6), (2021) 106544. https://doi.org/10.1016/j.jece.2021.106544

[6] A. Rasool, S. Sri, M. Zulfajri, F.S.H. Krismastuti, Nature inspired nanomaterials, advancements in green synthesis for biological sustainability. Inorganic Chemistry Communications, 169, (2024)112954. https://doi.org/10.1016/j.inoche.2024.112954

[7] H.N. Jayasimha, K.G. Chandrappa, P.F. Sanaulla, V.G. Dileepkumar, Green synthesis of CuO nanoparticles: A promising material for photocatalysis and electrochemical sensor. Sensors International, 5, (2024) 100254. https://doi.org/10.1016/j.sintl.2023.100254

[8] F.T. Thema, E. Manikandan, M.S. Dhlamini, M.J.M.L. Maaza, Green synthesis of ZnO nanoparticles via Agathosma betulina natural extract. Materials Letters, 161, (2015) 124-127. https://doi.org/10.1016/j.matlet.2015.08.052

[9] M. Ramesh, M. Anbuvannan, G. Viruthagiri, Green synthesis of ZnO nanoparticles using Solanum nigrum leaf extract and their antibacterial activity. Spectrochimica Acta Part A: Molecular and Biomolecular Spectroscopy, 136, (2015). 864-870. https://doi.org/10.1016/j.saa.2014.09.105

[10] P. Prabu, V. Losetty, Green synthesis of copper oxide nanoparticles using Macroptilium Lathyroides (L) leaf extract and their spectroscopic characterization, biological activity and photocatalytic dye degradation study. Journal of Molecular Structure, 1301, (2024) 137404. https://doi.org/10.1016/j.molstruc.2023.137404

[11] A. Suba, P. Selvarajan, J.J. Devadasan, Rubidium chloride doped magnesium oxide nanomaterial by using green synthesis and its characterization. Chemical Physics Letters, 793, (2022) 139463. https://doi.org/10.1016/j.cplett.2022.139463

[12] J. Xu, Y. Huang, S. Zhu, N. Abbes, X. Jing, L. Zhang, A review of the green synthesis of ZnO nanoparticles using plant extracts and their prospects for application in antibacterial textiles. Journal of Engineered Fibers and Fabrics, 16, (2021). https://doi.org/10.1177/15589250211046242

[13] F. Davar, A. Majedi, A. Mirzaei, Green synthesis of ZnO nanoparticles and its application in the degradation of some dyes. Journal of the American Ceramic Society, 98(6), (2015) 1739-1746. https://doi.org/10.1111/jace.13467

[14] U.O. Aigbe, O.A. Osibote, Green synthesis of metal oxide nanoparticles, and their various applications. Journal of hazardous materials advances, 13, (2024) 100401. https://doi.org/10.1016/j.hazadv.2024.100401

[15] A. Wasilewska, U. Klekotka, M. Zambrzycka, G. Zambrowski, I. Święcicka, B. Kalska-Szostko, Physico-chemical properties and antimicrobial activity of silver nanoparticles fabricated by green synthesis. Food chemistry, 400, (2023) 133960. https://doi.org/10.1016/j.foodchem.2022.133960

[16] S. Varshney, A. Gupta, Forest industrial biomass residue-mediated green synthesized multifunctional copper oxide nanoparticles for efficient wastewater treatment and biomedical applications. Journal of Cleaner Production, 434, (2024) 140109. https://doi.org/10.1016/j.jclepro.2023.140109

[17] R. Kumar, K. Kumar, N. Thakur, A. Umar, A.A. Ibrahim, S. Akbar, S. Baskoutas, Green synthesis and multifunctional properties of Cu/NiO nanocomposites using Commelina benghalensis leaf extract. Chemosphere, 362, (2024) 142805. https://doi.org/10.1016/j.chemosphere.2024.142805

[18] T.U.D. Thi, T.T. Nguyen, Y.D. Thi, K.H.T. Thi, B.T. Phan, K.N. Pham, (2020). Green synthesis of ZnO nanoparticles using orange fruit peel extract for antibacterial activities. RSC advances, 10(40), 23899-23907. https://doi.org/10.1039/D0RA04926C

[19] N. Kumari, P. Kumari, A.K. Jha, K. Prasad, Green synthesis of Cu2O nanoparticles using grape juice and its antimicrobial activity. In AIP Conference Proceedings, 2220(1), (2020). https://doi.org/10.1063/5.0002290

[20] G. Vasyliev, V. Vorobyova, Valorization of Food Waste to Produce Eco-Friendly Means of Corrosion Protection and "Green" Synthesis of Nanoparticles. Advances in Materials Science and Engineering, 2020(1), (2020) 6615118. https://doi.org/10.1155/2020/6615118

[21] N. Sedefoglu, Green synthesis of ZnO nanoparticles by Myrtus communis plant extract with investigation of effect of precursor, calcination temperature and study of photocatalytic performance. Ceramics International, 50(6), (2024) 9884-9895. https://doi.org/10.1016/j.ceramint.2024.01.387

[22] A. Shakerimoghaddam, H.J. Majeed, A. J. Hashim, M.J. Abed, L.S. Jasim, M. Salavati-Niasari, Green synthesis and characterization of NiO/Hydroxyapatite nanocomposites in the presence of peppermint extract and investigation of their antibacterial activities against Pseudomonas aeruginosa and Staphylococcus aureus. Results in Chemistry, 13 (2025). 101947. https://doi.org/10.1016/j.rechem.2024.101947

[23] M. Kaur, A. Gautam, P. Guleria, K. Singh, V. Kumar, Green synthesis of metal nanoparticles and their environmental applications. Current Opinion in Environmental Science & Health, 29, (2022) 100390. https://doi.org/10.1016/j.coesh.2022.100390

[24] K.M. Gendo, R. Feyisa Bogale, G. Kenasa, Green Synthesis, Characterization, and Evaluation of Photocatalytic and Antibacterial Activities of Co_3O_4–ZnO Nanocomposites Using Calpurnia aurea Leaf Extract. ACS omega, 9(26), (2024) 28354-28371. https://doi.org/10.1021/acsomega.4c01595

[25] S. Drummer, O. Mkhari, M. Chowdhury, Green synthesis of Co_3O_4 nanoparticles using spent coffee: Application in catalytic and photocatalytic dye degradation. Next Nanotechnology, 6, (2024) 100069. https://doi.org/10.1016/j.nxnano.2024.100069

[26] P. Papolu, A. Bhogi, Green synthesis of various metal oxide nanoparticles for the environmental remediation-An overview. Materials Today: Proceedings, 92(2), (2023) 924-927. https://doi.org/10.1016/j.matpr.2023.04.544

[27] J. Yadav, P. Chauhan, R.K. Rawat, S.K. Pathak, S. Srivastava, Syzygium aromaticum-mediated green synthesis of iron oxide nanoparticles for efficient heavy metal removal from aqueous solutions. Journal of the Indian Chemical Society, 101(8), (2024) 101201. https://doi.org/10.1016/j.jics.2024.101201

[28] A. Maria, I. Ahmad, S. Naeem, D. Husain, A.B. Patil, D.K. Halwar, A.V. Patil, Green synthesis and characterization of crystalline copper nanoparticles via sodium borohydride reduction towards enhanced gas sensing application. Journal of the Indian Chemical Society, 101(6), (2024) 101157. https://doi.org/10.1016/j.jics.2024.101157

[29] P.M.Y, Ansari, R.M. Muthukrishnan, R.I. Khan, C. Vedhi, S. A. Kader, Green synthesis of copper oxide nanoparticles using Amaranthus caudatus leaf extract and its non-enzymatic glucose sensor application. Applied Physics A, 129(11) (2023) 743. https://doi.org/10.1016/j.chphi.2023.100374

[30] C. Hano, B.H. Abbasi, Plant-based green synthesis of nanoparticles: Production, characterization and applications. Biomolecules, 12(1), (2021) 31. https://doi.org/10.3390/biom12010031

[31] M. Khan, F. Ahmad, J.T. Koivisto, M. Kellomäki, Green synthesis of controlled size gold and silver nanoparticles using antioxidant as capping and reducing agent. Colloid and Interface Science Communications, 39, (2020) 100322. https://doi.org/10.1016/j.colcom.2020.100322

[32] I.S. Saputra, E. Nurfani, A.G. Fahmi, A.H. Saputro, D.O.B. Apriandanu, D. Annas, Y. Yulizar, Effect of secondary metabolites from several leaf extracts on the green synthesized-ZnO nanoparticles. Vacuum, 227, (2024) 113434. https://doi.org/10.1016/j.vacuum.2024.113434

[33] S. Kumar, A. Tahira, M. Emo, B. Vigolo, A. Infantes-Molin, A.M. Alotaibi, S.F. Shaikh, A. NafadyIbupoto, Z. Hussain Ibupoto, Grapefruit juice containing rich hydroxyl and oxygenated groups capable of transforming 1D structure of NiCo2O4 into 0D with excessive surface vacancies for promising energy conversion and storage applications. Journal of Energy Storage, 68, (2023) 107708. https://doi.org/10.1016/j.est.2023.107708

[34] J. Meena, S. Shankari Sivasubramaniam, E. David, Green supercapacitors: review and perspectives on sustainable template-free synthesis of metal and metal oxide nanoparticles. RSC Sustainability, 2(5), (2024) 1224-1245. https://doi.org/10.1039/D4SU00009A

[35] H.M. Abuzeid, C.M. Julien, L. Zhu, A.M. Hashem, Green synthesis of nanoparticles and their energy storage, environmental, and biomedical applications. Crystals, 13(11), (2023) 1576. https://doi.org/10.3390/cryst13111576

[36] E.T. Bekele, Y.D. Sintayehu, B.A. Gonfa, F.K. Sabir, M.K. Shumete, C.R. Ravikumar, N. Kumar H.A. Murthy, Green synthesis of ternary ZnO/ZnCo2O4 nanocomposites using Ricinus communis leaf extract for the electrochemical sensing of sulfamethoxazole. Inorganic Chemistry Communications, 160, (2024) 111964. https://doi.org/10.1016/j.inoche.2023.111964

[37] L. Yadeta Gemachu, A. Lealem Birhanu, Green synthesis of ZnO, CuO and NiO nanoparticles using Neem leaf extract and comparing their

photocatalytic activity under solar irradiation. Green Chemistry Letters and Reviews, 17(1), (2024) 2293841. https://doi.org/10.1080/17518253.2023.2293841

[38] P.Raji, Green synthesis and characterization of Copper oxide nanoparticles using Luffa acutangula peel extract and its antibacterial activity. Results in Surfaces and Interfaces, 16, (2024) 100261. https://doi.org/10.1016/j.rsurfi.2024.100261

[39] M. Gowtham, Chandrasekar Sivakumar, Narendhar Chandrasekar, S. Balachandran, N. Senthil Kumar, Exploring Zinc Vanadate/Cobalt Oxide ($Zn_3(VO_4)_2$/CoO) Nano Hybrid Composites as Supercapacitors for Sustainable Energy Storage Applications, International Research Journal of Multidisciplinary Technovation, 6(3) (2024) 128-143. https://doi.org/10.54392/irjmt24310

[40] S. Kharat, S. Dahiwale, S.N. Inamdar, M.P. Shinde, Synthesis of cobalt oxide nanoparticles coated with carbon and its catalytic applications in organic reactions. Materials Today: Proceedings, 92, (2023) 1034-1039. https://doi.org/10.1016/j.matpr.2023.05.005

[41] K. Ali, M. Sajid, S.A. Bakar, A. Younus, H. Ali, M.Z. Rashid, Synthesis of copper oxide (CuO) via coprecipitation method: Tailoring structural and optical properties of CuO nanoparticles for optoelectronic device applications. Hybrid Advances, 6, (2024) 100250. https://doi.org/10.1016/j.hybadv.2024.100250

[42] C. Ramalechume, P. Shamili, R. Krishnaveni, C.M.A. Swamidoss, Synthesis of copper oxide nanoparticles using tree gum extract, its spectral characterization, and a study of its anti-bactericidal properties. Materials Today: Proceedings, 33, (2020) 4151-4155. https://doi.org/10.1016/j.matpr.2020.06.587

[43] D. Rajalakshmi, S. Gunasekaran, P.J. Paneerselvam, I. Kostova, Synthesis, characterization, and biomedical potential of nickel oxide and Silver-doped nickel oxide nanoparticles via green synthesis method. Physica B: Condensed Matter, 693, (2024) 416237. https://doi.org/10.1016/j.physb.2024.416237

[44] K.G. Devi, A.C. Dhanemozhi, & L.S. Priya, Green synthesis of Zinc oxide nanoparticles using lemon extract for waste water treatment. Materials Today: Proceedings (2023). https://doi.org/10.1016/j.matpr.2023.03.576

Authors Contribution Statement

S.J. Nilofur Fathima: Methodology, Investigation, Formal Analysis, Data curation, Writing original draft. C. Arun Paul: Writing Review & Editing. K. Mathu Metha: Writing Review & Editing. E. Ranjith Kumar: Conceptualization, Methodology, Investigation, Supervision, Formal Analysis, Data curation, Writing original draft. All the authors read and agreed the final version of the manuscript.

Funding

The authors declare that no funds, grants or any other support were received during the preparation of this manuscript.

Competing Interests

The authors declare that there are no conflicts of interest regarding the publication of this manuscript.

Data Availability

The data supporting the findings of this study can be obtained from the corresponding author upon reasonable request.

Has this article screened for similarity?

Yes